Journal of Organometallic Chemistry, 456 (1993) 271–278

JOM 23590

Mechanistic study of the reaction of $Os_3(CO)_{10}(CNPr)(NCMe)$ with Brønsted acid

Chi-Jung Su [a,b], Min-Ling Chung [a,b], Han-Mou Gau [b], Yuh-Sheng Wen [a] and Kuang-Lieh Lu [a]

[a] *Institute of Chemistry, Academia Sinica, Taipei (Taiwan, ROC)*

[b] *Department of Chemistry, National Chung-Hsing University, Taichung (Taiwan, ROC)*

(Received January 8, 1993; in revised form February 5, 1993)

Abstract

The reaction of $Os_3(CO)_{10}(CNPr)(NCMe)$ (**1**) with Brønsted acid in CH_2Cl_2 takes place initially via the protonation of **1** to yield the hydrido complex $[(\mu\text{-}H)Os_3(CO)_{10}(CNPr)(NCMe)]^+$ (**2**), followed by substitution of labile acetonitrile ligand with carboxylate anion to form the monodentate carboxylate complexes $(\mu\text{-}H)Os_3(CO)_{10}(CNPr)(\eta^1\text{-}OCOR)$ (**3**). Spectroscopic and crystallographic evidence is presented to explain mechanistic details of the reaction. Molecular structures of $(\mu\text{-}H)Os_3(CO)_{10}(CNPr)(\eta^1\text{-}OCOCF_3)$ (**3a**) and $(\mu\text{-}H)Os_3(CO)_{10}(CNPr)(\eta^1\text{-}OCOC \equiv CH)$ (**3b**) have been determined by X-ray diffraction studies. Crystal data: **3a**: $P2_1/n$; $a = 11.6632(19)$, $b = 14.7827(24)$, $c = 14.487(3)$ Å; $\beta = 103.635(15)°$, $V = 2427.4(7)$ Å^3, $Z = 4$, $R = 5.2\%$, $R_w = 5.4\%$. **3b**: $P3_2$; $a = 14.853(3)$, $c = 9.158(3)$ Å; $V = 1749.6(7)$ Å^3, $Z = 3$, $R = 3.2\%$, $R_w = 3.8\%$.

1. Introduction

Cluster complexes have been proved to possess low-energy pathways leading to reactions with high product selectivity [1]. Mechanistic studies of ligand addition and substitution are essential for a detailed analysis of stoichiometric or catalytic processes involving transition metal cluster complexes [2]. In a previous attempt to understand the effect of isocyanide-carbonyl replacement on the reactivity of metal isocyanide complexes, we developed a facile route to the preparation of osmium isocyanide clusters $Os_3(CO)_{11}(CNR)$ by an ylide-type reaction [3–4], and synthesized the "lightly stabilized" complexes $Os_3(CO)_{10}(CNR)(NCMe)$ as precursor to explore their reactions with propynoic acid [5]. Here we describe two crystal structures of the products $(\mu\text{-}H)Os_3(CO)_{10}(CNPr)(\eta^1\text{-}OCOR)$ ($R = CF_3$, $HC{\equiv}C$) and several pieces of evidence which elucidate the mechanistic details of these reactions.

2. Results and discussion

The reaction of complex $Os_3(CO)_{10}(CNPr)(NCMe)$ (**1**) with Brønsted acids in CH_2Cl_2 was suggested to proceed via the protonation of $Os_3(CO)_{10}(CNPr)$-(NCMe) to yield the hydrido complex $[(\mu\text{-}H)Os_3$-$(CO)_{10}(CNPr)(NCMe)]^+$ (**2**) at the first stage, followed by substitution of the labile nitrile ligand with carboxylate anion to form $(\mu\text{-}H)Os_3(CO)_{10}(CNPr)(\eta^1\text{-}OCOR)$ (**3**) with a terminal unidentate η^1-oxo mode. (Scheme 1). Some pieces of evidence to account for the reaction pathway are presented below.

Treatment of $Os_3(CO)_{10}(CNPr)(NCMe)$ (**1**) with $HBF_4 \cdot Et_2O$ or CF_3SO_3H in CH_2Cl_2 gives complexes formulated as $[(\mu\text{-}H)Os_3(CO)_{10}(CNPr)(NCMe)]^+X^-$ (**2a**, $X^- = BF_4^-$; **2b**, $X^- = CF_3SO_3^-$). Although the counter anions (BF_4^- and $CF_3SO_3^-$) are different, these two products showed the same IR spectrum in the ν(CO) stretching region (2118w, 2090vs, 2075s, 2037s cm^{-1}), implying these two protonated products bear the same cation $[(\mu\text{-}H)Os_3(CO)_{10}(CNPr)(NCMe)]^+$. In addition, the ν(CO) stretching of **2** shifts to higher

---

Correspondence to: Dr. K.-L. Lu.

0022-328X/93/$6.00

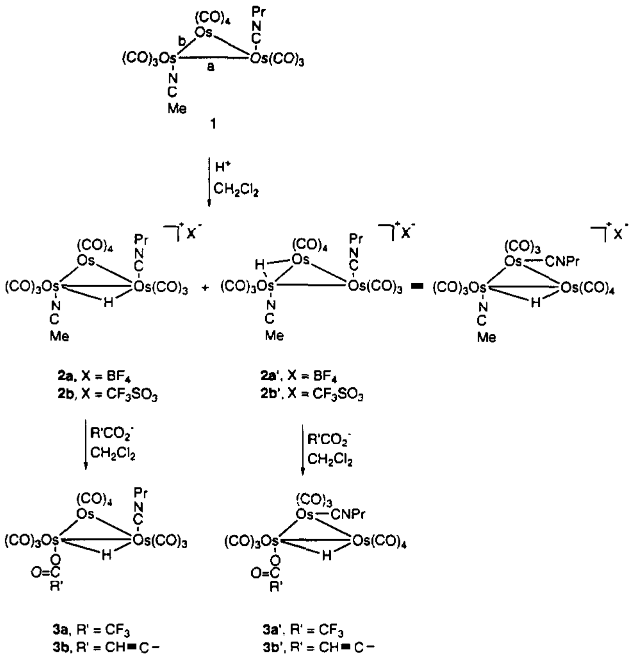

Scheme 1.

frequency for 67 cm^{-1} but retains a pattern integrity similar to that of $Os_3(CO)_{10}(CNPr)(NCMe)$, suggesting that the skeleton of the protonated metal clusters is analogous to that of the parent complex $Os_3(CO)_{10}(CNPr)(NCMe)$. The shift of $\nu(CO)$ stretching to higher frequency is due to the positive charge of the protonated complex **2**. A similar observation was detected in the reaction of $Os_3(CO)_{11}(NCMe)$ with HX [6], and an ionic derivative of a related type was also observed in the reaction of $Os_3(CO)_{12}$ with HX [7]. The IR spectrum of **2a** showed that a $\nu(CN)$ absorption appeared at 2231 cm^{-1}, which is characteristic of the terminally coordinated isocyanide ligand [8].

The ^1H NMR spectra of the products from the reactions of $Os_3(CO)_{10}(CNPr)(NCMe)$ with $HBF_4 \cdot Et_2O$ or CF_3SO_3H are nearly the same. The ^1H NMR spectrum of **2a** showed a methyl signal of coordinated acetonitrile resonating at δ 2.67, and two bridging hydride peaks at δ −16.57 and −16.66 in a 20:1 ratio, indicating that the complex exists as two isomeric forms. The protonation of complex **1** is likely to take place in a regiospecific fashion allowing the intermediate to exist in two isomeric forms. Two possibilities for protonation may occur on different sites in complex **1** as shown in Scheme 1: The site *a* located between two Os atoms bearing the electron donating isocyanide and nitrile ligand is likely to be the most preferred position for protonation to generate the major isomer **2**. On the

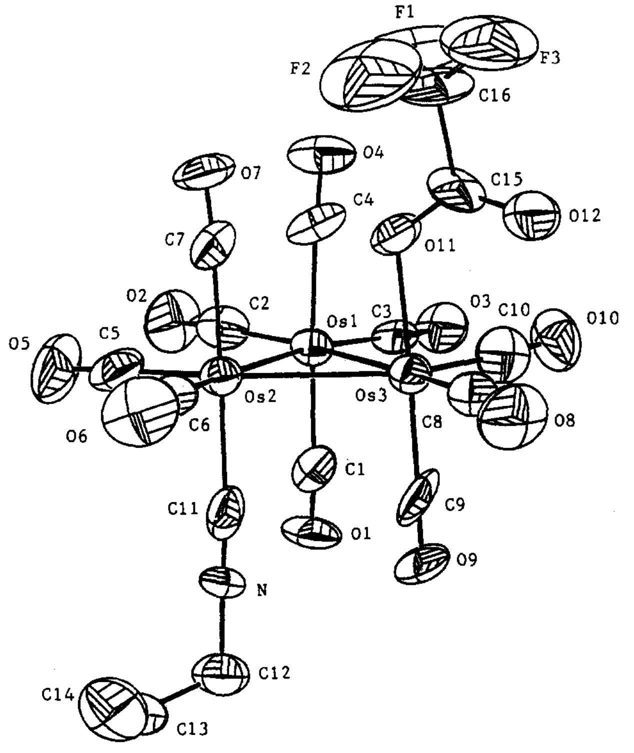

Fig. 1. ORTEP diagram of $(\mu\text{-H})Os_3(CO)_{10}(CNPr)(\eta^1\text{-OCOCF}_3)$ (**3a**).

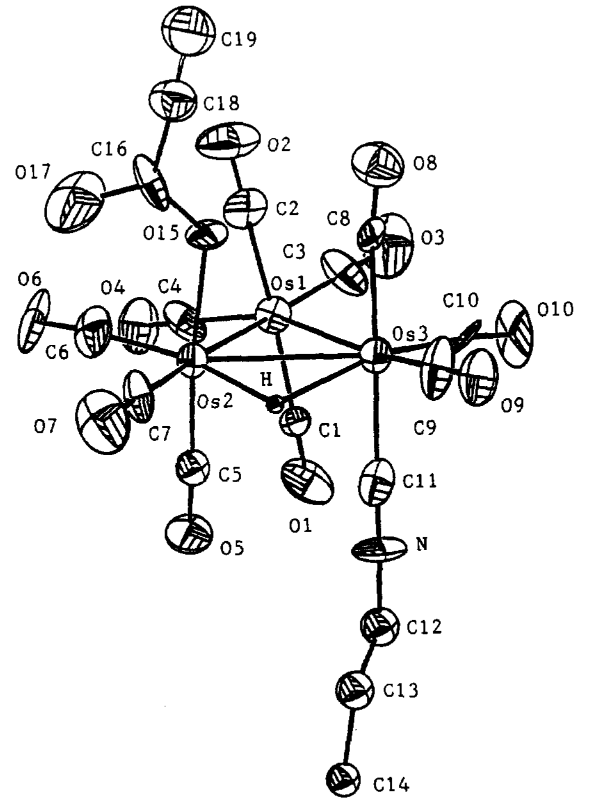

Fig. 2. ORTEP diagram of $(\mu\text{-H})Os_3(CO)_{10}(CNPr)(\eta^1\text{-OCOC≡CH})$ (**3b**).

other hand, the site *b* between $Os(CO)_3(NCMe)$ and $Os(CO)_4$ is suggested to be the second preferred site for protonation to afford the minor isomer **2′**.

Treatment of $Os_3(CO)_{10}(CNPr)(NCMe)$ with 1-2 equiv of CF_3CO_2H in CH_2Cl_2 at room temperature gives complex $(\mu\text{-H})Os_3(CO)_{10}(CNPr)(\eta^1\text{-OCOCF}_3)$ (**3a**). An X-ray crystal analysis of complex **3a** was undertaken (Fig. 1). The molecule consists of a triangular cluster of osmium atoms with distances Os(1)–Os(2) = 2.8890(11) Å, Os(1)–Os(3) = 2.8619(13) Å, and Os(2)–Os(3) = 2.9967(11) Å. The linear isocyanide ligand occupies an axial coordination site on Os(2) as observed in several other isocyanide metal carbonyl compounds [5,9]. The trifluoroacetate ligand coordinates axially on Os(3) with a terminal unidentate η^1-oxo coordination mode, demonstrating that the trifluoroacetate anion substitutes the labile acetonitrile ligand to form complex **3a**. Bridging hydride ligands are known to have significant lengthening effect on the metal–metal bond [10], thus we predict that the bridging hydride ligand straddles the Os(2)–Os(3) bond since this bond is substantially longer than the other two. The slight tilt of the trifluoroacetate ligand, with an Os(2)–Os(3)–O(11) angle of 84.2 (4)°, implies that a weak interaction probably remains between Os(3) and O(12) of the trifluoroacetate ligand. The IR spectrum of **3a** showed two absorption bands in the $\nu(CO_2)$, stretching region at 1684 and 1401 cm^{-1}. The separation between $\nu_{as}(CO_2)$ and $\nu_s(CO_2)$ frequencies (283 cm^{-1}) is substantially greater than that of CF_3CO_2Na (223 cm^{-1}) or CF_3CO_2K (241 cm^{-1}) [11,12], indicating that the coordinated trifluoroacetate is arranged as a unidentate carboxylate mode according to the criterion $[\Delta_{\text{unidentate}} > \Delta_{\text{ionic}}$; Δ is the separation between $\nu_{as}(CO_2)$ and $\nu_s(CO_2)]$ reported by Deacon [13]. This is consistent with the structure defined by X-ray diffraction study. Trifluroacetate ligand was also observed to bind terminally to the metal atom in a unidentate (η^1-oxo) mode in other complexes [14]. Compared to the weakly coordinated BF_4^- and $CF_3SO_3^-$ ligands, the $CF_3CO_2^-$ anion shows a slightly stronger coordination ability [15] to substitute the labile CH_3CN ligand of intermediate **2**, leading to the formation of complex **3a**.

The reaction of complex $Os_3(CO)_{10}(CNPr)(NCMe)$ (**1**) with $CH{\equiv}CCO_2H$ in CH_2Cl_2 affords complex $(\mu\text{-H})Os_3(CO)_{10}(CNPr)(\eta^1\text{-OCOC}{\equiv}\text{CH})$ (**3b**). An X-ray crystal analysis of complex **3b** was undertaken recently in order to obtain unambiguous information of its molecular stereochemistry (Fig. 2). This structure shows the complex containing a terminal unidentate (η^1-oxo)

TABLE 1. Crystal and intensity collection data for $(\mu\text{-H})Os_3(CO)_{10}(CNPr)(\eta^1\text{-OCOCF}_3)$ (**3a**) and $(\mu\text{-H})Os_3(CO)_{10}(CNPr)(\eta^1\text{-OCOC}{\equiv}\text{CH})$ (**3b**)

Formula	$C_{16}H_8F_3NO_{12}Os_3$	$C_{17}H_9NO_{12}Os_3$
F.W.	1033.83	989.85
Space group	$P2_1/n$	$P3_2$
a, Å	11.6632(19)	14.853(3)
b, Å	14.7827(24)	
c, Å	14.487(3)	9.158(3)
β, deg	103.635(15)	
V, Å^3	2427.4(7)	1749.6(7)
D_{calc}, g cm^{-3}	2.829	2.818
Z	4	3
Cryst. dimension, mm	0.38 × 0.19 × 0.44	0.46 × 0.31 × 0.38
Abs. coeff. μ(Mo Kα), mm^{-1}	15.76	18.38
Temp.	Room temperature	Room temperature
Radiation	Mo Kα	Mo Kα
2θ (max)	44.9°	44.8°
Scan type	θ–2θ	θ–2θ
Total no. of reflctn.	3353	1729
No. of observed reflctn.	2477 $F_o > 2\sigma(F_o)$	1410 $F_o > 2.5\sigma(F_o)$
Observed variables	316	278
R	0.052	0.032
R_w	0.054	0.038
$\Delta(\rho)$, e Å^{-3}	3.460	1.220
Δ/σ_{max}	0.498	0.180
GOF	2.50	1.69

carboxylate ligand rather than our previously suggested bridging unidentate (μ_2-η^1-oxo) mode [5]. Basically, this structure of **3b** is similar to that of complex **3a**. The bridging hydride which was observed crystallographically coordinates between Os(2) and Os(3) in accord with the elongation of Os(2)–Os(3) bond [2.9982(20) Å]. The isocyanide moiety bonds to Os(3) at the axial position. The carboxylate ligand is coordinated at Os(2) with a terminal unidentate (η^1-oxo) mode. The isocyanide and the carboxylate ligands are *trans* to each other with respect to the triosmium plane. Two C–O bonds [1.24(4) and 1.25(4) Å] in carboxylate ligand are near the same length, and C(18)–C(19) with a distance of 1.14(6) Å is a typical C–C triple bond. According to the criterion reported by Deacon [13], complex **3b** was suggested to contain a unidentate carboxylate group based on the absorption peaks in the $\nu(CO_2)$ region [$\Delta_{\text{unidentate}} = 311$ cm^{-1}, $\Delta_{\text{ionic}} = 199$ cm^{-1}]. However, this evidence from the IR spectrum alone is not sufficient to predict precisely whether the carboxylate ligand is coordinated as terminal unidentate or bridging unidentate modes. The X-ray diffraction study shows that the coordinated oxygen of carboxylate group in complex **3b** is unable to attack the vicinal Os atom to form the bridging unidentate (μ_2-η^1-oxo) coordination mode. Complexes containing similar η^1-oxo carboxylate mode were also observed in literature [16].

Treatment of $[(\mu\text{-H})Os_3(CO)_{10}(CNPr)(NCMe)]^+$ BF_4^- (**2a**) with excess $CH{\equiv}CCO_2^-Na^+$ yields mainly the hydrido complex $(\mu\text{-H})Os_3(CO)_{10}(CNPr)(\eta^1\text{-}OCOC{\equiv}CH)$ (**3b**) and the very minor bridging aminocarbyne complex $Os_3(CO)_{10}(\mu_2\text{-CNHPr})(\mu_2\text{-}OCOC{\equiv}CH)$ (**4**). In comparison with BF_4^-, the stronger nucleophile $CH{\equiv}CCO_2^-$ readily substitutes the acetonitrile ligand in intermediate **2** to afford $(\mu\text{-H})Os_3(CO)_{10}(CNPr)(\eta^1\text{-}OCOC{\equiv}CH)$ (**3b**). This reaction provides convincing evidence that complex **2** is the intermediate for the formation of complex **3** as shown in Scheme 1. The formation of traces of the bridging aminocarbyne complex **4** is probably due to the isomerization of **3b** induced by the excess of the base $CH{\equiv}CCO_2^-$. A related example of isomerization of $H_2Os_3(CO)_{10}$ (CNR) to $HOs_3(CO)_{10}(\mu\text{-CNHPr})$ catalyzed by base has been reported previously [8,17].

The ^1H NMR spectrum showed that complex $(\mu\text{-H})Os_3(CO)_{10}(CNPr)(\eta^1\text{-}OCOCF_3)$ exists as two isomeric forms (**3a** and **3a′**) with hydride resonance at δ −15.02 and δ −15.09 in a 10:1 ratio. In addition, complex $(\mu\text{-H})Os_3(CO)_{10}(CNPr)(\eta^1\text{-}OCOC{\equiv}CH)$ exhibits a similar pair (**3b** and **3b′**) of hydride peaks at δ − 15.07, −15.23 in a 10:3 ratio in its ^1H NMR spectrum as reported previously [5]. Complex **2** also exists as two isomers implying that the site preference for protonation of the starting material $Os_3(CO)_{10}$(CNPr)(NCMe) (**1**) may be responsible for the final configuration of products.

On the basis of the above observations, the reactions of $Os_3(CO)_{10}$(CNPr)(NCMe) with Brønsted acids most likely proceed by two distinct steps. Protonation is regarded as the initial step in the process, followed by subsequent replacement of labile acetonitrile by carboxylate anion to yield the final products $(\mu\text{-H})Os_3(CO)_{10}(CNPr)(\eta^1\text{-OCOR})$.

3. Experimental section

3.1. General data

Complexes $Os_3(CO)_{11}$(CNPr) and $Os_3(CO)_{10}$(CNPr)(NCMe) were prepared previously [3,5]. Other

TABLE 2. Atomic coordinates and isotropic thermal parameters (Å^2) for $(\mu\text{-H})Os_3(CO)_{10}(CNPr)(\eta^1\text{-}OCOCF_3)$ (**3a**)

Atom	*x*	*y*	*z*	B_{iso} [a]
Os1	0.76735(8)	0.84507(5)	0.99971(6)	3.51(4)
Os2	0.87141(8)	0.70170(5)	1.12780(6)	3.40(4)
Os3	0.86292(8)	0.89310(5)	1.19401(6)	3.64(4)
N	1.1284(14)	0.7359(10)	1.0939(12)	4.1(9)
F1	0.4691(16)	0.8466(16)	1.2372(14)	13.8(15)
F2	0.5633(20)	0.7682(12)	1.3363(18)	15.6(17)
F3	0.5232(19)	0.8766(16)	1.3806(15)	15.3(17)
O1	1.0098(14)	0.8812(10)	0.9531(12)	6.2(9)
O2	0.6866(18)	0.7261(11)	0.8240(11)	7.6(11)
O3	0.6855(15)	1.0333(9)	0.9237(12)	6.5(10)
O4	0.5213(14)	0.8230(11)	1.0421(13)	7.2(10)
O5	0.8266(18)	0.5621(10)	0.9662(12)	7.9(11)
O6	0.9867(17)	0.5749(10)	1.2922(13)	7.9(11)
O7	0.6241(14)	0.6552(10)	1.1557(12)	6.1(9)
O8	0.9818(17)	0.9244(12)	1.4050(11)	7.7(11)
O9	1.0979(14)	0.9404(9)	1.1562(12)	6.0(9)
O10	0.7733(17)	1.0841(9)	1.1440(13)	7.0(11)
O11	0.6979(13)	0.8529(9)	1.2226(10)	5.1(8)
O12	0.7064(15)	0.9552(10)	1.3424(12)	6.5(9)
C1	0.9274(22)	0.8692(13)	0.9761(17)	5.2(12)
C2	0.7117(21)	0.7707(14)	0.8875(16)	5.2(12)
C3	0.7202(21)	0.9625(13)	0.9559(17)	5.4(13)
C4	0.6117(22)	0.8265(15)	1.0318(18)	6.2(13)
C5	0.8406(21)	0.6140(13)	1.0244(17)	5.3(12)
C6	0.9420(21)	0.6202(14)	1.2293(17)	5.4(12)
C7	0.7108(20)	0.6757(12)	1.1434(15)	4.5(11)
C8	0.9296(21)	0.9125(13)	1.3259(17)	5.0(12)
C9	1.0146(24)	0.9241(13)	1.1699(17)	6.0(13)
C10	0.8118(23)	1.0117(13)	1.1664(15)	5.6(13)
C11	1.0411(20)	0.7278(12)	1.1073(15)	4.7(10)
C12	1.2460(21)	0.7474(15)	1.0818(18)	5.9(14)
C13	1.3056(22)	0.6559(16)	1.0842(19)	6.4(14)
C14	1.320(3)	0.6075(16)	1.1756(21)	8.2(17)
C15	0.6651(22)	0.8891(15)	1.2944(15)	5.3(13)
C16	0.5472(23)	0.8508(19)	1.3067(17)	7.0(15)

[a] B_{iso} is the mean of the principal axes of the thermal ellipsoid.

reagents were purchased from commercial sources and were used as received. All manipulations were performed under a nitrogen atmosphere using standard Schlenk techniques. Solvents were dried by stirring over CaH_2 (hexane, CH_2Cl_2, CH_3CN) and were freshly distilled prior to use. IR spectra were recorded on a

TABLE 3. Selected bond distances (Å) and angles (deg) for (μ-H)$Os_3(CO)_{10}$(CNPr)(η^1-$OCOCF_3$) (**3a**)

(a) Bond distances			
Os(1)-Os(2)	2.8890(11)	O(1)-C(1)	1.10(3)
Os(1)-Os(3)	2.8619(13)	O(2)-C(2)	1.11(3)
Os(1)-C(1)	2.01(3)	O(3)-C(3)	1.18(3)
Os(1)-C(2)	1.943(23)	O(4)-C(4)	1.10(3)
Os(1)-C(3)	1.885(22)	O(5)-C(5)	1.12(3)
Os(1)-C(4)	2.00(3)	O(6)-C(6)	1.15(3)
Os(2)-Os(3)	2.9967(11)	O(7)-C(7)	1.11(3)
Os(2)-C(5)	1.950(23)	O(8)-C(8)	1.18(3)
Os(2)-C(6)	1.929(24)	O(9)-C(9)	1.06(3)
Os(2)-C(7)	1.976(23)	O(10)-C(10)	1.18(3)
Os(2)-C(11)	2.106(25)	O(11)-C(15)	1.304(24)
Os(3)-O(11)	2.146(14)	O(12)-C(15)	1.23(3)
Os(3)-C(8)	1.907(24)	C(12)-C(13)	1.52(3)
Os(3)-C(9)	1.94(3)	Os(3)-C(10)	1.865(23)
N-C(11)	1.09(3)	C(13)-C(14)	1.48(4)
N-C(12)	1.43(3)	F(1)-F(2)	1.97(3)
F(1)-F(3)	2.07(3)	F(1)-C(16)	1.19(3)
F(2)-F(3)	1.83(3)	F(2)-C(16)	1.29(3)
C(15)-C(16)	1.54(3)	F(3)-C(16)	1.23(3)
(b) Bond angles			
Os(2)-Os(1)-Os(3)	62.81(3)	Os(2)-Os(1)-C(1)	88.5(6)
Os(2)-Os(1)-C(2)	97.4(6)	Os(2)-Os(1)-C(3)	159.5(7)
Os(2)-Os(1)-C(4)	91.0(7)	Os(3)-Os(1)-C(1)	87.8(6)
Os(3)-Os(1)-C(2)	159.9(6)	Os(3)-Os(1)-C(3)	96.8(7)
Os(3)-Os(1)-C(4)	88.3(7)	Os(3)-O(11)-C(15)	119.0(13)
C(1)-Os(1)-C(2)	95.7(10)	Os(1)-C(1)-O(1)	172.4(20)
C(1)-Os(1)-C(3)	89.3(9)	Os(1)-C(2)-O(2)	175.7(22)
C(1)-Os(1)-C(4)	175.8(9)	Os(1)-C(3)-O(3)	175.6(21)
C(2)-Os(1)-C(3)	103.1(9)	Os(1)-C(4)-O(4)	172.2(21)
C(2)-Os(1)-C(4)	88.5(10)	Os(2)-C(5)-O(5)	177.6(22)
C(3)-Os(1)-C(4)	89.8(9)	Os(2)-C(6)-O(6)	176.8(19)
Os(1)-Os(2)-Os(3)	58.15(3)	Os(2)-C(7)-O(7)	174.6(18)
Os(1)-Os(2)-C(5)	91.2(6)	Os(3)-C(8)-O(8)	173.2(21)
Os(1)-Os(2)-C(6)	170.8(6)	Os(3)-C(9)-O(9)	179.3(18)
Os(1)-Os(2)-C(7)	87.1(6)	Os(3)-C(10)-O(10)	175.3(21)
Os(1)-Os(2)-C(11)	92.4(5)	Os(2)-C(11)-N	175.3(16)
Os(3)-Os(2)-C(5)	149.3(6)	N-C(12)-C(13)	109.7(18)
Os(3)-Os(2)-C(6)	112.7(6)	Os(3)-Os(2)-C(7)	92.5(5)
Os(3)-Os(2)-C(11)	88.6(5)	C(5)-Os(2)-C(6)	98.0(9)
C(5)-Os(2)-C(7)	87.2(9)	C(5)-Os(2)-C(11)	91.3(9)
C(6)-Os(2)-C(7)	92.1(9)	C(6)-Os(2)-C(11)	88.6(9)
C(7)-Os(2)-C(11)	178.4(8)	Os(1)-Os(3)-Os(2)	59.04(3)
Os(1)-Os(3)-O(11)	87.8(4)	Os(1)-Os(3)-C(8)	174.3(6)
Os(1)-Os(3)-C(9)	92.4(6)	Os(1)-Os(3)-C(10)	89.5(6)
Os(2)-Os(3)-O(11)	84.2(4)	Os(2)-Os(3)-C(8)	115.2(6)
Os(2)-Os(3)-C(9)	93.8(6)	Os(2)-Os(3)-C(10)	148.4(7)
O(11)-C(15)-O(12)	128.9(21)	O(11)-Os(3)-C(8)	91.2(8)
O(11)-C(15)-C(16)	112.3(19)	O(11)-Os(3)-C(9)	177.5(8)
O(12)-C(15)-C(16)	118.0(20)	O(11)-Os(3)-C(10)	92.6(8)
F(1)-C(16)-F(2)	104.7(25)	C(8)-Os(3)-C(9)	88.3(10)
F(1)-C(16)-F(3)	117(3)	C(8)-Os(3)-C(10)	96.2(9)
F(1)-C(16-C(15)	116.6(20)	C(9)-Os(3)-C(10)	89.9(10)
F(2)-C(16)-F(3)	92.8(22)	C(11)-N-C(12)	176.8(22)
F(2)-C(16)-C(15)	108.9(23)	F(2)-F(1)-F(3)	53.7(11)
F(3)-C(16)-C(15)	112.4(22)		

Perkin-Elmer 882 infrared spectrophotometer. NMR spectra were obtained on a Bruker MSL-200, an AC-200 or an AMX-500 FT NMR spectrometer, and mass spectra were recorded on a VG 70-250S mass spectrometer. Elemental analyses were performed using a Perkin-Elmer 2400 CHN elemental analyzer.

3.2. *Reaction of* $Os_3(CO)_{10}(CNPr)(NCMe)$ *with* $HBF_4 \cdot Et_2O$ *and* CF_3SO_3H

A solution of $Os_3(CO)_{11}(CNPr)$ (30 mg, 0.03 mmol) in CH_2Cl_2 (30 ml) and acetonitrile (1 ml) was treated with a solution of Me_3NO (3 mg, 0.04 mmol) in 20:100 CH_3CN/CH_2Cl_2 (3 ml). The mixture was stirred for 30 min at room temperature and filtered through a short silica column. The solvent was removed under vacuum, and the residue was dissolved in 20 ml of CH_2Cl_2. The resulting solution of $Os_3(CO)_{10}(CNPr)(NCMe)$ was treated with excess $HBF_4 \cdot Et_2O$ (0.02 ml, 0.15 mmol) and stirred for 10 min. The solvent was removed under vacuum to furnish $[(\mu\text{-H})Os_3(CO)_{10}(CNPr)(NCMe)]^+BF_4^-$ (**2a**) with more than 80% NMR yield. The IR spectrum showed that the reaction proceeded almost quantitatively. Attempts to grow a single crystal of **2a** for X-ray study were not successful. IR (CH_2Cl_2): $\nu(CN) = 2231$w, $\nu(CO) = 2118$ w, 2090 vs, 2075s, 2036s cm^{-1}. ^1H NMR ($CDCl_3$): δ 3.91 (t, 2H, $CNCH_2$), 2.67 (s, 3H, $NCCH_3$), 1.74 (m, 2H, CH_2), 1.00 (t, 3H, CH_3), −16.57, −16.66 (s, 1H, Os–H–Os, two isomers in a 20:1 ratio).

Complex **2b** was obtained under reaction conditions similar to those of **2a** using CF_3SO_3H as reagent. Data for $[(\mu\text{-H})Os_3(CO)_{10}(CNPr)(NCMe)]^+CF_3SO_3^-$ (**2b**) are as follows. IR (CH_2Cl_2): $\nu(CN) = 2230$w, $\nu(CO) =$ 2118w, 2090vs, 2075s, 2037s cm^{-1}. ^1H NMR ($CDCl_3$): δ 3.91 (t, 2H, $CNCH_2$), 2.72 (s, 3H, $NCCH_3$), 1.74 (m, 2H, CH_2), 1.00 (t, 3H, CH_3), −16.51, −16.60 (s, 1H, Os–H–Os, two isomers in a 20:1 ratio).

3.3. *Reaction of* $Os_3(CO)_{10}(CNPr)(NCMe)$ *with* CF_3CO_2H

A solution of $Os_3(CO)_{11}(CNPr)$ (54 mg, 0.06 mmol) in CH_2Cl_2 (60 ml) and acetonitrile (1 ml) was treated with a solution of Me_3NO (8 mg, 0.08 mmol) in 20:100 CH_3CN/CH_2Cl_2 (3 ml). The mixture was stirred for 30 min at room temperature and filtered through a small silica column. The solvent was removed under vacuum, and the residue was dissolved in 60 ml of CH_2Cl_2. The resulting solution of $Os_3(CO)_{10}(CNPr)$ (NCMe) was treated with CF_3CO_2H (9 μl, 0.08 mmol) and stirred for 10 min. The solvent was removed under vacuum, and the residue was chromatographed on a silica gel TLC plate with 50:50 CH_2Cl_2/hexane as eluent to give $(\mu\text{-H})Os_3(CO)_{10}(CNPr)(\eta^1\text{-}OCOCF_3)$ (**3a**) (36 mg, 0.04 mmol, 61%). Anal. Calcd for $C_{16}H_8F_3NO_{12}Os_3$: C, 18.58; H, 0.77. Found: C, 18.85; H, 0.74%. IR (CH_2Cl_2): $\nu(CN) = 2228$w, $\nu(CO) =$ 2113w, 2084vs, 2069s, 2043m, 2022s, 2013 sh, 1983br cm^{-1} [$\nu(CO_2) = 1684$, 1401 cm^{-1} in KBr]. ^1H NMR ($CDCl_3$): δ 3.86, 3.74 (t, 2H, CH_2, $J(HH) = 6.9$ Hz, two isomers), 1.75 (m, 2H, CH_2), 1.01 (t, 3H, CH_3, $J(HH) = 7.2$ Hz), −15.02, −15.09 (s, 1H, Os–H–Os, two isomers in a 10:1 ratio). MS (FAB): m/z 1033 (M^+).

3.4. *Reaction of* $[(\mu\text{-H})Os_3(CO)_{10}(CNPr)(NCMe)]^+BF_4^-$ *with* $HC{\equiv}CCO_2^-Na^+$

A solution of $Os_3(CO)_{11}(CNPr)$ (30 mg, 0.03 mmol) in CH_2Cl_2 (30 ml) and acetonitrile (1 ml) was treated with a solution of Me_3NO (4 mg, 0.05 mmol) in 20:100 CH_3CN/CH_2Cl_2 (3 ml). The mixture was stirred for 30 min at room temperature and filtered through a

TABLE 4. Atomic coordinates and isotropic thermal parameters ($Å^2$) for $(\mu\text{-H})Os_3(CO)_{10}(CNPr)(\eta^1\text{-}OCOC{\equiv}CH)$ (**3b**)

Atom	x	y	z	B_{iso} [a]
Os1	0.23971(9)	0.43115(9)	0.62287	2.83(6)
Os2	0.23303(9)	0.33555(9)	0.89771(17)	2.48(6)
Os3	0.08809(9)	0.21285(9)	0.65461(17)	2.62(6)
N	−0.0886(23)	0.2481(27)	0.7922(35)	5.5(20)
O1	0.0589(23)	0.4687(18)	0.6832(27)	5.3(16)
O2	0.4291(21)	0.4038(20)	0.5752(34)	6.5(19)
O3	0.2295(25)	0.4556(23)	0.3014(40)	7.7(22)
O4	0.3785(19)	0.6588(18)	0.7226(29)	5.6(15)
O5	0.0895(19)	0.4121(21)	1.0042(29)	5.8(16)
O6	0.4227(19)	0.5358(21)	1.0030(31)	5.9(15)
O7	0.2143(22)	0.2328(21)	1.1833(29)	6.1(19)
O8	0.2513(20)	0.1769(18)	0.5159(26)	4.7(16)
O9	−0.0396(18)	−0.0215(17)	0.7018(24)	4.0(13)
O10	0.0071(24)	0.2187(26)	0.3515(28)	7.5(22)
O15	0.3207(15)	0.2690(16)	0.8135(22)	3.1(12)
O17	0.4527(23)	0.3463(24)	0.9611(39)	8.5(24)
C1	0.1231(22)	0.4472(23)	0.6663(34)	3.2(17)
C2	0.3557(25)	0.4100(20)	0.5975(38)	3.6(17)
C3	0.2336(31)	0.4462(27)	0.4269(40)	4.6(24)
C4	0.3294(30)	0.5744(29)	0.6895(31)	4.1(24)
C5	0.1435(23)	0.3827(23)	0.9580(30)	2.8(5)
C6	0.3551(29)	0.4607(29)	0.9596(36)	4.3(21)
C7	0.2209(25)	0.2659(24)	1.0795(30)	3.1(18)
C8	0.1970(20)	0.1962(21)	0.5714(29)	2.3(14)
C9	0.0094(27)	0.0640(27)	0.6873(40)	4.7(20)
C10	0.0406(20)	0.2164(24)	0.4576(41)	3.6(17)
C11	−0.0257(25)	0.2389(25)	0.7440(36)	3.9(18)
C12	−0.1577(36)	0.2891(36)	0.8293(52)	7.2(11)
C13	−0.2009(63)	0.2450(59)	0.9689(94)	14.2(24)
C14	−0.2733(31)	0.2773(30)	1.0472(43)	5.6(9)
C16	0.4067(31)	0.2865(24)	0.8575(32)	3.8(21)
C18	0.4451(28)	0.2194(29)	0.8026(37)	4.1(20)
C19	0.4816(31)	0.1738(33)	0.7557(42)	5.5(25)
H	0.112	0.213	0.882	2.7

[a] B_{iso} is the mean of the principal axes of the thermal ellipsoid.

small silica column. The solvent was removed under vacuum, and the residue was dissolved in 20 ml of CH_2Cl_2. The resulting solution of $Os_3(CO)_{10}(CNPr)(NCMe)$ was then treated with excess $HBF_4 \cdot Et_2O$ (0.04 ml, 0.34 mmol) and stirred for 10 min. The product $[(\mu\text{-H})Os_3(CO)_{10}(CNPr)(NCMe)]^+BF_4^-$ (**2a**) was treated with a suspension of excess $HC{\equiv}CCO_2^-Na^+$ in CH_2Cl_2 (20 ml) at room temperature. The IR spec-

TABLE 5. Selected bond distances (Å) and angles (deg) for $(\mu\text{-H})Os_3(CO)_{10}(CNPr)(\eta^1\text{-OCOC}{\equiv}CH)$ (**3b**)

(a) Bond distances			
Os(1)–Os(2)	2.8672(18)	O(4)–C(4)	1.13(5)
Os(1)–Os(3)	2.8926(17)	O(5)–C(5)	1.17(4)
Os(1)–C(1)	1.90(3)	O(6)–C(6)	1.14(4)
Os(1)–C(2)	1.91(4)	O(7)–C(7)	1.05(4)
Os(1)–C(3)	1.82(4)	O(8)–C(8)	1.11(4)
Os(1)–C(4)	1.96(4)	O(9)–C(9)	1.11(4)
Os(2)–Os(3)	2.9982(20)	O(10)–C(10)	1.10(4)
Os(2)–O(15)	2.135(17)	O(15)–C(16)	1.24(4)
Os(2)–C(5)	1.87(3)	O(17)–C(16)	1.25(4)
Os(2)–C(6)	1.92(4)	C(12)–C(13)	1.43(10)
Os(2)–C(7)	1.92(3)	Os(2)–H	1.82
Os(3)–C(8)	1.91(3)	C(13)–C(14)	1.55(9)
Os(3)–C(9)	1.94(4)	Os(3)–C(10)	1.95(4)
Os(3)–C(11)	2.08(4)	Os(3)–H	2.11
N–C(11)	1.10(5)	N–C(12)	1.47(6)
C(16)–C(18)	1.46(5)	O(1)–C(1)	1.16(4)
C(18)–C(19)	1.14(6)	O(2)–C(2)	1.16(4)
O(3)–C(3)	1.16(5)		
(b) Bond angles			
Os(2)–Os(1)–Os(3)	62.74(4)	C(8)–Os(3)–C(9)	88.9(14)
Os(2)–Os(1)–C(1)	94.0(10)	C(8)–Os(3)–C(10)	88.6(11)
Os(2)–Os(1)–C(2)	80.6(10)	C(8)–Os(3)–C(11)	177.2(12)
Os(2)–Os(1)–C(3)	159.5(10)	Os(2)–Os(1)–C(4)	95.8(8)
C(9)–Os(3)–C(10)	98.9(13)	Os(3)–Os(1)–C(1)	82.7(9)
C(9)–Os(3)–C(11)	94.0(15)	Os(3)–Os(1)–C(2)	95.1(8)
Os(3)–Os(1)–C(3)	100.3(11)	C(10)–Os(3)–C(11)	91.2(12)
Os(3)–Os(1)–C(4)	155.7(9)	C(1)–Os(1)–C(2)	174.6(14)
C(1)–Os(1)–C(3)	94.9(15)	C(11)–N–C(12)	162(4)
C(1)–Os(1)–C(4)	88.1(13)	Os(2)–O(15)–C(16)	126.2(18)
C(2)–Os(1)–C(3)	90.3(16)	Os(1)–C(1)–O(1)	171(3)
C(2)–Os(1)–C(4)	92.1(13)	Os(1)–C(2)–O(2)	174(3)
C(3)–Os(1)–C(4)	102.9(14)	Os(1)–C(3)–O(3)	179(3)
Os(1)–Os(2)–Os(3)	59.05(5)	Os(1)–C(4)–O(4)	176(3)
Os(1)–Os(2)–O(15)	92.0(5)	Os(2)–C(5)–O(5)	175(3)
Os(1)–Os(2)–C(5)	85.9(9)	Os(2)–C(6)–O(6)	174(3)
Os(1)–Os(2)–C(6)	89.9(10)	Os(2)–C(7)–O(7)	175(3)
Os(1)–Os(2)–C(7)	176.9(9)	Os(3)–C(8)–O(8)	172.1(24)
Os(3)–C(9)–O(9)	176(3)	Os(3)–Os(2)–O(15)	82.5(6)
Os(3)–C(10)–O(10)	174(3)	Os(3)–Os(2)–C(5)	91.0(9)
Os(3)–C(11)–N	176(3)	Os(3)–Os(2)–C(6)	148.2(10)
N–C(12)–C(13)	105(5)	Os(3)–Os(2)–C(7)	118.1(9)
Os(3)–Os(2)–H	43.95	O(15)–Os(2)–C(5)	173.3(10)
O(15)–Os(2)–C(6)	93.2(12)	O(15)–Os(2)–C(7)	88.7(11)
C(12)–C(13)–C(14)	119(6)	C(5)–Os(2)–C(6)	93.1(14)
C(5)–Os(2)–C(7)	93.1(13)	C(6)–Os(2)–C(7)	93.1(13)
Os(1)–Os(3)–Os(2)	58.22(4)	Os(1)–Os(3)–C(8)	82.5(8)
Os(1)–Os(3)–C(9)	168.9(10)	Os(1)–Os(3)–C(10)	88.1(9)
Os(1)–Os(3)–C(11)	94.6(9)	O(15)–C(16)–O(17)	122(3)
Os(2)–Os(3)–C(8)	88.7(8)	O(15)–C(16)–C(18)	117(3)
Os(2)–Os(3)–C(9)	114.8(10)	O(17)–C(16)–C(18)	119(3)
Os(2)–Os(3)–C(10)	146.2(9)	C(16)–C(18)–C(19)	174(4)
Os(2)–Os(3)–C(11)	89.9(8)	Os(2)–Os(3)–H	36.81
Os(2)–H–Os(3)	99.25		

trum showed that the transformation from **2a** to **3b** was completed in 5 h. The resulting solution was filtered, concentrated and chromatographed on a silica gel TLC plate with 50:50 CH_2Cl_2/hexane as eluent to give $(\mu\text{-H})Os_3(CO)_{10}(CNPr)(\mu_2\text{-OCOC}{\equiv}CH)$ (**3b**) (9 mg, 0.009 mmol, 28%) and $Os_3(CO)_{10}(\mu\text{-CNHPr})(\mu\text{-OCOC}{\equiv}CH)$ (**4**) (1 mg, 0.001 mmol, 3%).

3.5. Crystallographic structure determination of $(\mu\text{-H})Os_3(CO)_{10}(CNPr)(\eta^1\text{-OCOCF}_3)$ *(3a) and* $(\mu\text{-H})Os_3(CO)_{10}(CNPr)(\eta^1\text{-OCOC}{\equiv}CH)$ *(3b).*

Crystals **3a** and **3b** were grown from CH_2Cl_2/hexane solutions at -5°C. Specimens of suitable quality were mounted on a glass capillary and used for measurement of precise cell constants and intensity data collection. All diffraction measurements were made on an Enraf-Norius CAD-4 diffractometer using graphite-monochromatized Mo $K\alpha$ radiation ($\lambda = 0.70930$ Å) with θ–2θ scan mode. Unit cells were determined and refined using 25 randomly selected reflections obtained using the CAD-4 automatic search, centre, index and least-squares routines. Space groups were determined from the systematic absences observed during data collection. The systematic absences in the diffraction data of **3a** and **3b** unambiguously established the space group as $P2_1/n$ and $P3_2$, respectively. An empirical absorption correction was applied to each of the data sets. The structure of **3a** was solved by heavy-atom method, and **3b** was solved by direct method. All remaining non-hydrogen atoms were located from the difference Fourier map, and they were included in the final refinement cycle and refined by full-matrix least squares. All the data processing was carried out on a Microvax 3600 using the NRCC SDP program. Crystallographic data are shown in Table 1. Final atomic coordinates, isotropic thermal parameters, and selected bond distances and bond angles for two complexes are listed in Tables 2–5.

4. Supplementary material available

Tables of atomic coordinates, crystal and intensity collection data, anisotropic thermal parameters, and bond lengths and angles (10 pages), and tables of structure factors (19 pages) are available from the authors.

Acknowledgments

We thank the National Science Council of the Republic of China for financial support.

References

1 G. Lavigne and H.D. Kaesz, in B.C. Gates, L. Guczi and H. Knözinger (Eds.), *Metal Clusters in Catalysis*, Elsevier, Amsterdam, 1986.

2 (a) D. Daresbourg, in D.F. Shriver, H.D. Kaesz and R.D. Adams (Eds.), *The Chemistry of Metal Cluster Complexes*, VCH, New York, 1990; (b) A.J. Poé, in M. Moscowits (Ed.), *Metal Cluster*, Wiley-Interscience, New York, 1986; (c) R.D. Adams, Y. Chi, D.D. DesMarteau, D. Lentz and R. Marschall, *J. Am. Chem. Soc., 114* (1992) 1909.

3 (a) Y.W. Lin, H.M. Gau, Y.S. Wen and K.L. Lu, *Organometallics, 11* (1992) 1445; (b) K.L. Lu, C.C. Chen, Y.W. Lin, F.E. Hong, H.M. Gau, L.L. Gan and H.D. Luoh, *J. Organomet. Chem.*, in press.

4 L.C. Chen, M.Y. Chen, J.W. Chen, Y.S. Wen and K.L. Lu, *J. Organomet. Chem., 425* (1992) 99; (b) C.A. Mirkin, K.L. Lu, G.L. Geoffroy, A.L. Rheingold and D.L. Staley, *J. Am. Chem. Soc., 111* (1989) 7279; (c) C.A. Mirkin, K.L. Lu, T.E. Snead, B.A. Young, G.L. Geoffroy, A.L. Rheingold and D.L. Staley, *J. Am. Chem. Soc., 113* (1991) 3800; (d) J. Kiji, A. Matsumura, T. Haishi, S. Okazaki and J. Furukawa, *Bull. Chem. Soc. Jpn., 50* (1977) 2731; (e) H. Alper and R.A. Partis, *J. Organomet. Chem., 35* (1972) C40.

5 K.L. Lu, C.J. Su, Y.W. Lin, H.M. Gau and Y.S. Wen, *Organometallics, 11* (1992) 3832.

6 B.F.G. Johnson, J. Lewis and D.A. Pippard, *J. Chem. Soc., Dalton Trans.*, (1981) 407.

7 A.J. Deeming and M. Underhill, *J. Chem. Soc., Dalton Trans.*, (1974) 1415.

8 R.D. Adams and N.M. Golembeski, *J. Am. Chem. Soc., 101* (1979) 2579.

9 R.D. Adams and N.M. Golembeski, *Inorg. Chem., 18* (1979) 1909.

10 R.D. Adams and J.E. Babin, *Organometallics, 7* (1988) 963.

11 W. Klemperer and G.C. Pimentel, *J. Chem. Phys., 22* (1954) 1399.

12 C.D. Garner and B. Hughes, *Adv. Inorg. Chem. Radiochem., 17* (1975) 1.

13 (a) G.B. Deacon and R.J. Phillips, *Coord. Chem. Rev., 33* (1980) 227; (b) G.B. Deacon and F. Huber, *Inorg. Chim. Acta, 104* (1985) 41.

14 M.J. Chetcuti, J.C. Gordon, K.A. Green, P.E. Fanwick and D. Morgenstern, *Organometallics, 8* (1989) 1790.

15 G.R. Frauenhoff, S.R. Wilson and J.R. Shapley, *Inorg. Chem., 30* (1991) 78.

16 P. Frediani, M. Bianchi, F. Piacenti, S. Ianelli and M. Nardelli, *Inorg. Chem., 26* (1987) 1592.

17 (a) R.D. Adams, *Acc. Chem. Res., 16* (1983) 67; (b) E. Rosenberg, *Polyhedron, 8* (1989) 383.